

УДК 541.64:537.5

## DC CONDUCTION MECHANISM IN PLASMA POLYMERIZED VINYLENE CARBONATE THIN FILMS PREPARED BY GLOW DISCHARGE TECHNIQUE<sup>1</sup>

© 2011 г. Sunirmal Majumder and A. H. Bhuiyan

Department of Physics, Bangladesh University of Engineering and Technology (BUET), Dhaka-1000, Bangladesh  
e-mail: abhuiyan@phy.buet.ac.bd

Received April 28, 2010;

Revised Manuscript Received July 7, 2010

**Abstract**—Electrical glow discharge technique was employed for the preparation of plasma polymerized vinylene carbonate (PPVC) thin films of aluminum/thin film/aluminum sandwich structure at room temperature by a parallel plate capacitively coupled reactor. The structural investigation of the monomer VC and PPVC was performed by Fourier transform infrared spectroscopy. The current density-voltage characteristics follow a power law of the form  $J \propto V^n$ , where  $n$  has different values. In the low voltage region  $0.85 < n < 1.00$  and those in the high voltage region lie between  $1.30 < n < 1.75$ , indicating Ohmic current conduction in the low voltage region and non-Ohmic conduction in the high voltage region. In addition, at higher temperature the current density increased significantly revealing a temperature dependence of the current density. Theoretically calculated values and experimental results of Schottky and Poole–Frenkel coefficients show that the most probable conduction mechanism in the PPVC thin films is of Schottky type.

### INTRODUCTION

Plasma polymers have attained a distinct position in the field of new materials and industrialization due to their adaptable/controllable optical, thermal, electrical, and other properties [1–3]. The reason behind the increasing interest is, a large number of applications in a wide range of fields such as production of membranes for reverse osmosis [4], solar mirror protective coatings [5], thin films insulators and capacitors in integrated microelectronics [6, 7], biosensors [8], chemical sensors [9] and humidity sensors [10]. Researchers have chosen plasma polymerization technique due to its suitability as a dry method for the chip and microelectronics industry. Since last four decades a large number of studies have been performed on the thin polymeric films, yet these materials need further study to find high quality new materials for electrical, electronic, and optical based devices in industrial and scientific applications. Kipnusu et al. [11] reported Ohmic conduction in the low electric fields and space charge limited conduction (SCLC) in the high electric fields. Phonon assisted variable range hopping transport mechanism is dominant between two localized states in the temperature range of 330–440 K.

Nespurek et al. [12] briefly outlined the theory of SCLC mechanism in organic thin films. They reported that current-voltage ( $I-V$ ) characteristics strongly depend on temperature, presence of charge carrier traps, and their distribution in energy, spatial inhomogeneity of the sample and electrode configuration. The

presence of a trap influences generation-recombination noise which can be employed to determine density-of-states. Gulalkari et al. [13] suggested that Schottky–Richardson conduction mechanism to be applicable in polyvinylchloride (PVC)–poly(methyl methacrylate) (PMMA) blend films and absence of thermodynamic transition in the temperature range of 313–353 K. Deshmukh et al. [14] studied the electrical properties of polyaniline doped PVC–PMMA and suggested that neither Poole–Frenkel (PF) nor Fowler–Nordheim mechanisms could explain the conductivity, rather Schottky–Richardson mechanism could be applied closely in the temperature range of 323–363 K. Shah Jalal et al. [15] studied the conduction mechanism in plasma polymerized *m*-xylene (PPm-X) thin films and inferred that the PF type of conduction was most probable in PPm-X thin films. Akther and Bhuiyan [16] investigated the electrical conduction mechanism in plasma polymerized *N,N*,3,5-tetramethylaniline thin films and suggested that the conduction mechanism was SCLC. Pipinys et al. [17] performed experiments to establish a model for the conduction mechanism in polyethylene (PE) films under high electric fields. To ascertain the peculiar behavior they suggested a model based on phonon assisted tunneling of charge carriers from localized states to the conducting ones, enables them to explain the temperature dependent  $I-V$  characteristics both in PE films and other polymers. Thus it can be noticed that a variety of mechanisms are responsible for the electrical conduction in various materials depending on the history of preparation and processing.

<sup>1</sup> Статья печатается в представленном авторами виде.

The vinylene carbonate (VC) is a cyclic, reactive, unsaturated carbonate ester [18, 19]. The role of VC as an additive was studied and the solid electrolyte interfacial layer resulting from its reduction was characterized by infrared spectroscopy [20, 21]. The best use of VC is, as a component of surface coatings. Although there are reports on the additive characteristics of VC, as yet a scanty of study on the electrical properties of thin films obtained from VC has been appeared in the literature. The vinylene compounds have applications in the electrical and optical devices [18, 21]. So the investigations of the structural and electrical properties of thin films grown from VC are of necessity for its application in various devices. From this point of view, the studies of the structural and electrical properties of plasma polymerized vinylene carbonate (PPVC) thin films have been undertaken. In this paper, the structural characteristics by Fourier transform infrared (FTIR) analysis and the current density-voltage ( $J-V$ ) characteristics at different temperatures of the PPVC are presented.

## EXPERIMENTAL PROCEDURE

### *The monomer*

The VC ( $C_3H_2O_3$ ) (Technical grade, 97%, Aldrich Chemical Company, USA) in liquid form was used as an organic precursor. The chemical structure of the monomer is shown in Fig. 1 and the physical properties of VC are given in Table 1.

### *The Fourier transform infrared (FTIR) spectroscopy*

FTIR spectroscopic analysis was used for determining the presence or absence of specific functional groups in polymers. The FTIR spectra were recorded to investigate the chemical structure of the VC and PPVC.

### *The experimental set up for plasma polymerization*

A capacitively coupled reactor was used for deposition of PPVC. The reactor consists of three parts, namely, vacuum system, gas inlet system and discharge system. The glow discharge system has two parallel circular plates of stainless steel with a diameter of 0.09 m and thickness of 0.001 m placed 0.04 m apart. Prior to the polymerization process the glow discharge chamber was evacuated by a rotary pump down to a base pressure of 1.33 Pa. Plasma was generated in the chamber at the line frequency 50 Hz. During the reaction, a vacuum gauge was used to measure the pressure inside the plasma chamber. During polymerization the power of the glow discharge was kept at about 40 W and deposition was made for 60 minutes.

**Table 1.** Some physical properties of vinylene carbonate ( $C_3H_2O_3$ )

Name of the Property	Property
Form	Clear liquid
Color	Colorless
Molecular Formula	$C_3H_2O_3$
Molecular Weight	86.05
Boiling point	435 K
Flash point	346 K
Density	1.355 g/ml

### *Sample preparation for FTIR and electrical studies*

The FTIR spectrum of the monomer VC was obtained by putting the liquid monomer in a KBr measuring cell. The PPVC powder was collected from the PPVC deposited substrates and then pellets of PPVC powder mixed with KBr were prepared for recording the FTIR spectrum of PPVC. The FTIR spectra of the different samples were recorded at room temperature by using a double beam IR spectrophotometer (SHIMADZU FTIR-8900 spectrophotometer) in the wavenumber range of 400–4000  $cm^{-1}$ . The FTIR spectra of the VC monomer and the PPVC thin films were recorded in transmittance (%) mode. Glass slides (18 mm  $\times$  18 mm  $\times$  1 mm) (Sail brand, China) were used as substrates in this work. Before thin film deposition the substrates were cleaned very carefully with acetone and dried by high quality cotton. Again substrates were cleaned by distilled water in an ultrasonic bath. The cleaned glass slides were next rinsed with deionized water and then dried properly. Then the substrates were preserved in desiccators. Metal electrodes of aluminum (Al) for electrical measurements were deposited using an Edward coating unit E-306 A (Edward, UK). All of the components of the coating unit were properly cleaned with acetone. The process of deposition starts after achieving a vacuum, of the order of  $1.33 \times 10^{-3}$  Pa or better in the deposition chamber. The vacuum chamber was evacuated by an oil diffusion pump backed by an oil rotary pump. The glass substrates were masked with a 0.08 m  $\times$  0.08 m  $\times$  0.001 m engraved brass sheet for the electrode depo-

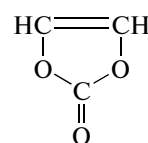


**Fig. 1.** The chemical structure of vinylene carbonate.

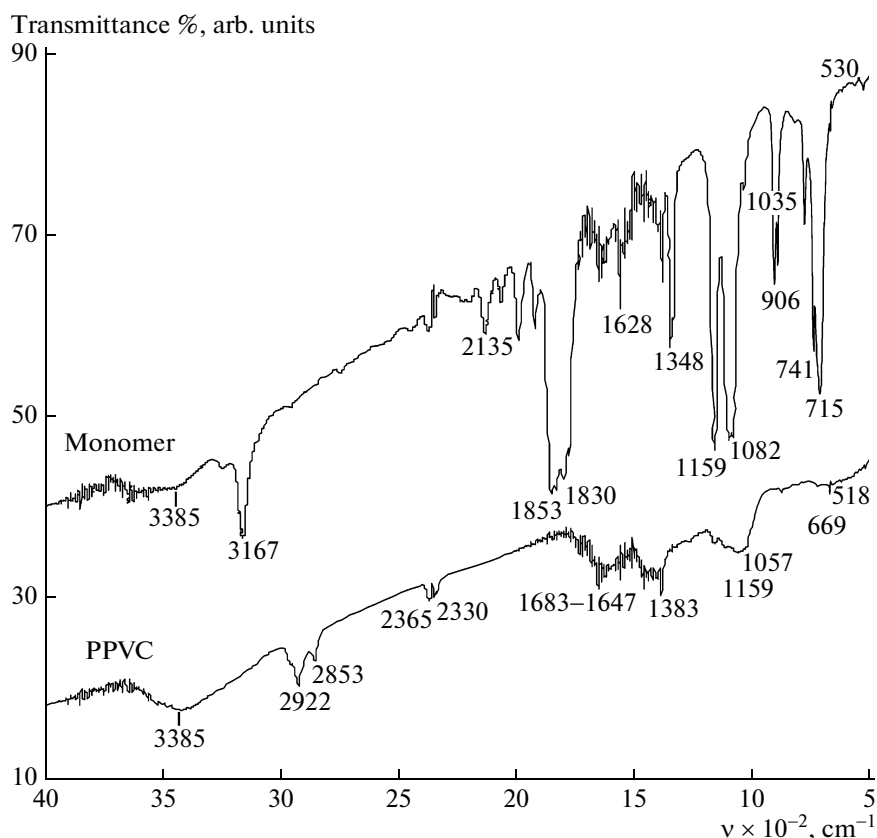


Fig. 2. The FTIR spectra of monomer VC and PPVC.

sition. For the electrode deposition Al was kept on the tungsten filament. The filament was heated by low-tension power supply of the coating unit. During evacuation of the chamber by diffusion pump, the diffusion unit was cooled by the flow of chilled

water and its outlet temperature was not allowed to rise above 305 K. When the Penning gauge reads about  $1.33 \times 10^{-3}$  Pa, the Al on the tungsten filament was heated by low-tension power supply until it was evaporated.

**Table 2.** Assignments of IR absorption peaks for monomer vinylene carbonate (VC) and plasma polymerized vinylene carbonate (PPVC)

Types of vibration/Assignments	Vinylene Carbonate Wave number [21], $\text{cm}^{-1}$	Vinylene Carbonate Wave number, $\text{cm}^{-1}$	PPVC Wave number, $\text{cm}^{-1}$
O–H stretch	3245	3385	3385
Symmetric C–H stretch	3170	3167	2922, 2853
C≡C stretch	2130	2135	2365, 2330
C=O stretch	1831	1853, 1830	1869
Skeletal (C=C) stretch	1620	1628	1683–1647
C–H in-plane bend	1347	1348	1383
C–H in-plane bend	1160	1159	1159
Skeletal (C–O) stretch	1081	1082, 1035	1057
Skeletal breathing	905	906	
Skeletal bend	740	741	
C–H out-of-plane	711	715	669
C=O out-of-plane	532	530	518

## RESULTS AND DISCUSSION

*The Fourier transform infrared analyses*

Figure 2 represents the FTIR spectra of the VC monomer and the PPVC recorded at room temperature and the peak assignments of the spectra are presented in Table 2. The FTIR spectrum of the VC monomer is in good agreement with previously published literature [21]. From the previous recorded data [21] it is observed that VC has 18 vibration fundamentals which can be classified according to the four irreducible representations. In the monomer spectrum a strong peak is observed at  $3167\text{ cm}^{-1}$ , close to  $3170\text{ cm}^{-1}$  is due to symmetric C–H stretching. Another peak is observed at  $1830\text{ cm}^{-1}$  due to C=O stretching. A skeletal stretch (C=C) peak is observed at  $1628\text{ cm}^{-1}$ . At  $1348\text{ cm}^{-1}$  a strong peak is observed due to C–H in-plane bending. At  $1160\text{ cm}^{-1}$  a peak is observed due to C–H in-plane bending. A strong peak at  $1082\text{ cm}^{-1}$  is due to skeletal (C–O) stretching and at  $906\text{ cm}^{-1}$  may be assigned to skeletal (C–O) breathing. The peak observed at  $741\text{ cm}^{-1}$  corresponds to skeletal (C–O) bend. A very strong peak at  $715\text{ cm}^{-1}$  is due to C–H out-of-plane. A very small peak at  $530\text{ cm}^{-1}$  is due to C=O out-of-plane [21].

A comparison of the FTIR spectra of the VC and PPVC revealed that the spectrum of the VC is changed to some extent after formation of the PPVC. In the FTIR spectrum of the PPVC thin films a broad band is observed around  $3385\text{ cm}^{-1}$  due to O–H bond, which may arise due to absorbed moisture from air. A peak is observed at  $2922\text{ cm}^{-1}$  corresponds to aromatic ring C–H stretching and C is a part of ring. The C=C and C=N are assigned to the wavenumber range  $2300\text{--}2000\text{ cm}^{-1}$ . In the spectrum of PPVC two medium strong peaks are observed at  $2330$  and  $2365\text{ cm}^{-1}$  which may be assigned to the formation of C=C due to abstraction of hydrogen during plasma deposition. In the VC spectrum a strong peak is observed at  $2135\text{ cm}^{-1}$ . Due to symmetry a terminal C=C produces a stronger band than an internal C=C (pseudosymmetry) [22]. At the wavenumber  $1869\text{ cm}^{-1}$  a very weak peak is observed, which may be due to C=O stretching. Generally C=O and C=C are assigned in the wavenumber range  $1900\text{--}1500\text{ cm}^{-1}$  [22].

The VC is unsaturated cyclic ester and esters have two characteristically strong absorption bands originated from C=O and C–O stretching. The C=O stretching vibration occurs at higher frequencies. The force constant of the carbonyl bond is increased by the electron attracting nature of the adjacent oxygen atom (inductive effect). The C=O absorption band of saturated aliphatic esters is in the region of  $1750\text{--}1735\text{ cm}^{-1}$ . The C=O absorption band of unsaturated esters are in the region of  $1730\text{--}1715\text{ cm}^{-1}$ . In the spectra of vinyl or phenyl esters, with unsaturation adjacent to the C–O group, a marked rise in the carbonyl

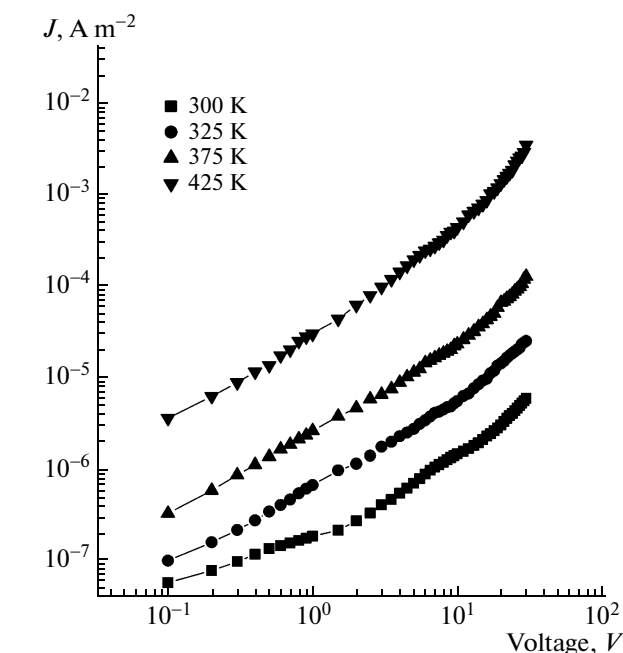


Fig. 3. Variation of current density with applied voltage at different temperatures for PPVC thin film (thickness,  $d = 130\text{ nm}$ ).

frequency is observed along with a lowering of the C–O frequency [22]. Vinyl acetate has a carbonyl bond at  $1776\text{ cm}^{-1}$  whereas VC has an absorption band at  $1830\text{ cm}^{-1}$  [22], but in the PPVC this band appears at  $1869\text{ cm}^{-1}$  corresponding to C=O stretching. At the wavenumber  $1653\text{ cm}^{-1}$  a medium peak is observed due to deformation of aromatic C=C stretching close to assigned wavenumber  $1620\text{ cm}^{-1}$ . In the range  $1660\text{--}1730\text{ cm}^{-1}$  the unclear peaks indicating that during plasma polymerization C=O may be broken. Also in the FTIR spectrum of the VC a large number of sharp peaks are observed in the lower wavenumber region whereas in that of the PPVC diffused peaks are observed with a clear one at  $1383\text{ cm}^{-1}$ , which is assigned to C–H in-plane bending. In the region  $1160\text{ cm}^{-1}$  a small peak is observed due to C–H plane bend. At  $1057\text{ cm}^{-1}$ , a broad band is observed which may be due to C–O skeletal stretch. A shifting to shorter/longer wavelengths diminishing the peaks/bands significantly in the PPVC spectrum compared to that of the VC spectrum indicate the occurrence of fragmentation of the monomer during plasma polymerization. Therefore structural modification occurs due to hydrogen abstraction/fragmentation and cross linking of the VC structure.

*The J–V characteristics*

For a specific polymeric material one of the four different conduction mechanisms will be dominant. The probable conduction mechanisms named as

**Table 3.** Values of 'n' at different temperatures for PPVC samples with thickness 130 nm

Temperature, K	Values of the slopes	
	Low voltage region	High voltage region
300	1.00	1.30
325	1.00	1.45
375	0.85	1.55
425	1.00	1.75

SCLC, electrode limited Schottky type conduction, bulk limited PF conduction and tunneling. Figure 3 represents the  $J$ - $V$  characteristics curves of a PPVC thin film of 130 nm thickness at the temperatures of 300, 325, 375 and 425 K. The variation of  $J$  with  $V$  seems to be linear in the low voltage region, but at higher voltages, the rate of increase of current density is faster. The  $J$ - $V$  characteristics follow a power law of the form  $J \propto V^n$  with different 'n' values (slopes). In the low voltage region the values of slope are  $0.85 < n < 1.00$  and that of in the high voltage region lie between  $1.30 < n < 1.75$  as shown in Table 3.

So these observations indicate that the current conduction is Ohmic in the low voltage region and non-Ohmic in the high voltage region. In addition, at the higher temperatures the current density increases significantly, revealing a strong temperature dependence of the current density. The steady-state space-charge-limited conduction current density,  $J$ , in a plane-par-

allel dielectric sample with an electrode separation  $d$  is proportional to the square of the applied voltage  $V$ . That is, the current density obeys an equation of the form [23]

$$J = \frac{9\epsilon\epsilon_0\mu V^2}{8d^3}, \quad (1)$$

where  $\epsilon$  is the dielectric constant of the material,  $\epsilon_0$  is the permittivity of the free space and  $\mu$  is the mobility of charge carriers. Therefore, for SCLC mechanism the slope of the  $J$ - $V$  characteristics should be greater than or equal to 2.

From the  $J$ - $V$  plots in Fig. 3 it is observed that in the higher voltage region the calculated values of the slopes are much smaller than that required for SCLC. Actually, in the higher voltage region, the slopes are less than 2, which suggest the possibility of PF or Schottky type mechanisms in the PPVC thin films and the possibility of SCLC is negligible. Tunneling is another possible conduction mechanism but for very thin film of thickness of the order of a few nanometers. The sample used in the present measurement is far away from this range. So there is no possibility of tunneling effect.

The general expression for both Schottky and PF type conduction is expressed by the equation of the form [24]

$$J = J_0 \exp\left(\frac{\beta F^{1/2} - \phi}{kT}\right), \quad (2)$$

where  $J_0$  is the low-field current density,  $F$  is the applied electric field,  $k$  is the Boltzmann constant,  $T$  is the absolute temperature and  $\phi$  is the ionization energy of localized centers in PF conduction and Coulomb barrier height of the electrode polymer interface in Schottky type conduction,  $\beta$  is the coefficient of the static electric field. The coefficient  $\beta$  for the Schottky type conduction is known as Schottky coefficient,  $\beta_s$ , and defined as

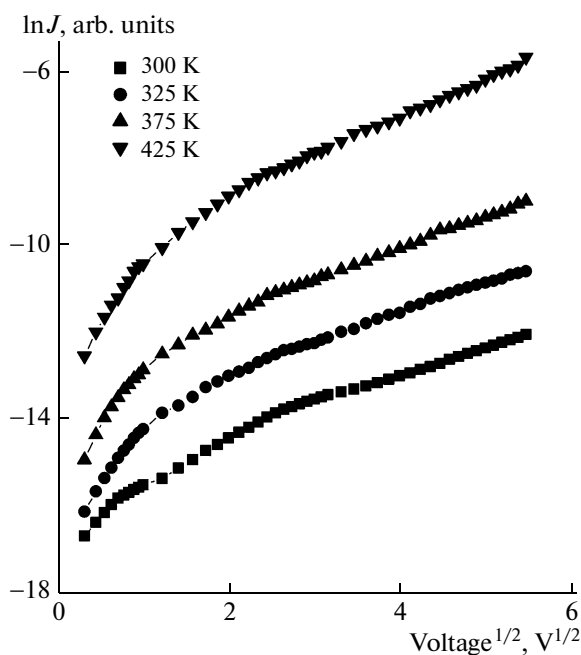
$$\beta_s = \left(\frac{e^3}{4\pi\epsilon\epsilon_0}\right)^{1/2}. \quad (3)$$

For the PF mechanism, it is called the PF coefficient,  $\beta_{PF}$ , and is defined as

$$\beta_{PF} = 2\left(\frac{e^3}{4\pi\epsilon\epsilon_0}\right)^{1/2} = 2\beta_s, \quad (4)$$

where  $e$  is the electronic charge.

So, according to equation (2) a plot of  $\ln J$  versus  $V^{1/2}$  (Schottky plots) should be a straight line in the higher voltage region with a positive slope [14]. Figure 4 shows the plots between  $\ln J$  versus  $V^{1/2}$  for a PPVC thin film of thickness 130 nm. It is observed from the Fig. 4 that Schottky plots are approximately straight line with positive slopes indicating the probable conduction mechanism to be of Schottky or PF type. Therefore, from the voltage dependence current density data at different elevated temperatures it is found

**Fig. 4.** Variation of  $\ln J$  with square root of applied voltage for PPVC thin film (thickness,  $d = 130$  nm) [Schottky plots].

**Table 4.** Comparison between the theoretical and experimental  $\beta$  coefficients with thickness 130 nm

Dielectric constant	Temperature, K	Theoretical, $\beta_{th}$		Experimental, $\beta_{exp}$ ( $eV\cdot m^{1/2} V^{-1/2}$ )
		$\beta_S$ ( $eV\cdot m^{1/2} V^{-1/2}$ )	$\beta_{PF}$ ( $eV\cdot m^{1/2} V^{-1/2}$ )	
6.00	300	$1.55 \times 10^{-5}$	$3.10 \times 10^{-5}$	$0.60 \times 10^{-5}$
5.38	325	$1.64 \times 10^{-5}$	$3.28 \times 10^{-5}$	$0.70 \times 10^{-5}$
4.93	375	$1.71 \times 10^{-5}$	$3.42 \times 10^{-5}$	$0.85 \times 10^{-5}$
4.89	425	$1.72 \times 10^{-5}$	$3.44 \times 10^{-5}$	$1.20 \times 10^{-5}$

that the mechanism of charge transport in PPVC may be due to Schottky or PF type.

To differentiate between these two possible mechanisms Schottky coefficient ( $\beta_s$ ) and PF coefficient ( $\beta_{PF}$ ) should be calculated theoretically and compared with the  $\beta$  found experimentally. To calculate experimental values of the  $\beta$  coefficients the relation  $\beta_{exp} = skTd^{1/2}$  were used, where  $s$  is the slope ( $s = \Delta \ln J / \Delta V^{1/2}$ ) of the graph plotted between  $\ln J$  and  $V^{1/2}$ . The theoretical values of the coefficients were calculated from the equations (3) and (4).

From the Table 4 it is clearly seen that the experimental values are very close to the theoretically calculated Schottky coefficient which indicates that the probable mechanism of charge transport in the PPVC thin film is of Schottky type. Furthermore in Schottky–Richardson mechanism, the current density shows strong temperature dependence but not in the case of PF mechanism [14]. Therefore an alternative way to identify whether the conduction mechanism is

PF or Schottky, it is appropriate to investigate the temperature dependence of the current density. To affirm Schottky–Richardson mechanism  $\ln(J/T^2)$  vs.  $1/T$  curve should be a straight line with a negative slope [25].

Figure 5 shows the plot of  $\ln(J/T^2)$  vs.  $1/T$  (Richardson plots) for the PPVC thin film of thickness 130 nm. It is observed from the Fig. 5 that at two fixed voltages (5 and 20 V) the curves are straight line indicating the Schottky type conduction mechanism. So, the conduction mechanism in the PPVC thin films has a maximum possibility of being Schottky type. The straight line with constant slope observed throughout the applied electric field indicating the absence of any thermodynamic transition with in the measured temperature range.

## CONCLUSIONS

The comparative study of the FTIR spectra of VC and PPVC yields that the PPVC thin films grown by plasma polymerization technique have slightly different chemical structure from that of the VC due to some structural rearrangement. The absence and/or shifting of some of the FTIR absorption bands in the PPVC support the above observations. From the  $J$ – $V$  characteristics of PPVC thin films it is observed that the current increases nonlinearly with the applied voltage. With a fixed voltage, the current densities are higher at higher temperatures. Theoretically calculated values and experimental results of  $\beta_s$  and  $\beta_{PF}$  have lead to comment on the conduction mechanism as Schottky type. The temperature dependence of current density also suggests Schottky type mechanism. Therefore it may be concluded that the most probable conduction mechanism in the PPVC thin films is of Schottky type.

## ACKNOWLEDGMENTS

One of authors, S. Majumder, acknowledges the financial support offered by the authority of Bangladesh University Grant Commission, Agargaon, Dhaka-1207 as a Ph. D. fellowship and also to the Ministry of Education, Bangladesh for sanctioning 3 years deputation for higher study.

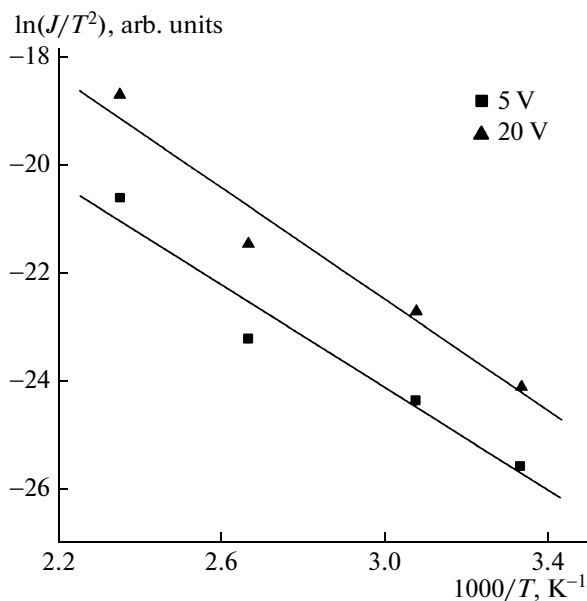


**Fig. 5.** Variation of  $\ln(J/T^2)$  with inverse absolute temperature for PPVC thin film (thickness,  $d = 130$  nm) [Richardson plots].

## REFERENCES

1. H. Yasuda, *Plasma Polymerization* (Acad. Press, Orlando, 1985).
2. *Plasma Deposition, Treatment and Etching of Polymers*, Ed. by R. d'Agostino (Academic Press, San Diego, CA, 1990).
3. F. F. Shi and J. M. S. Rev, *Macromol. Chem. Phys.* **C36** (4), 795 (1996).
4. M. S. Silverstein and I. Visoly-Fisher, *Polymer* **43**, 11 (2002).
5. H. Biederman and Y. Osada, "Plasma Chemistry of Polymers," *Advance in Polymer Science* **95**, 57 (1990).
6. J. M. Tibbitt, A. T. Bell, and M. Shen, *J. Macromol. Sci.-Chem.* **A10**, 519 (1976).
7. G. Sawa, O. Ito, S. Morita, and M. Ieda, *J. Polym. Sci. Polym. Phys. Ed.* **12**, 1231 (1974).
8. H. Muguruma, *Tr. Anal. Chem.* **19**, 433 (2007).
9. M. Nakamura, L. Sugimoto, and H. Kuwano, *Sens. Actuators B: Chem.* **33**, 122 (1998).
10. N. Guermat, A. Bellel, S. Sahli, Y. Segui, and P. Raynaud, *Thin Solid Films* **517**, 4455 (2009).
11. W. K. Kipnusu, G. Katana, C. M. Migwi, I. V. S. Rathore, and J. R. Sangoro, *Int. J. Biomats. Article 2009 ID 548406* (2009).
12. S. Nespurek, O. Zmeskal, and J. Sworakowski, *Thin Solid Films* **516**, 8949 (2008).
13. R. S. Gulalkari, Y. G. Bakale, D. K. Burghate, and V. S. Deogaonkar, *Pramana-J. Phys.* **69**, 485 (2007).
14. S. H. Deshmukh, D. K. Burghate, V. P. Akhare, V. S. Deogaonkar, P. T. Deshmukh, and M. S. Deshmukh, *Bull. Mater. Sci.* **30**, 51 (2007).
15. A. B. M. Shah Jalal, S. Ahmed, A. H. Bhuiyan, and M. Ibrahim, *Thin Solid Films* **295**, 125 (1997).
16. H. Akther and A. H. Bhuiyan, *Thin Solid Films* **488**, 93 (2005).
17. P. Pipinys, A. Rimeika, and V. Lapeika, *J. Phys. D: Appl. Phys.* **37**, 828 (2004).
18. X. Zhang, T. J. Richardson, J. K. Pugh, and P. N. Ross, *J. Electrochem. Soc.* **148**(12), A1341-A1345 (2001).
19. G. R. Slayton, J. W. Simmons, and J. H. Goldstein, *J. Chem. Phys.* **22**(10), 1678 (1954).
20. H. Hu, W. Kong, H. Li, H. Huang, and L. Chen, *Electrochem. Comm.* **6**, 126 (2004).
21. L. K. Dorris, E. J. Boggs, A. Danti, and L. L. Altpeter, *J. Chem. Phys.* **46**(3), 1191 (1967).
22. M. R. Silverstein, C. G. Bassler, and C. T. Morrill, *Spectrometric Identification of Organic Compounds* (John Wiley and Sons, New York, 1981).
23. N. F. Mott and R. W. Gurney, *Electronic Processes in Ionic Crystals* (Clarendon Press, Oxford, 1940), p. 168.
24. J. G. Simmons, "Electronic Conduction Through Thin Insulating Films", in *Handbook of Thin Film Technology*, Ed. by L. I. Maissel and R. Glang (McGraw-Hill, New York, 1970), p. 1425.
25. Po-Tsun Liu, T. C. Chang, Shuo-Ting Yau, Chun-Huai Li, and S. M. Sze, *J. Electrochem. Soc.* **150** (2), F7-F10 (2003).